A MINIATURIZED AEROSOL SENSOR IMPLEMENTED BY A SILICON-BASED MEMS THERMAL-PIEZORESISTIVE OSCILLATOR

Chia-Chun Chu[1], Ting-Yuan Liu[1], Tzu-Ming Chen[2], Chien-Hao Weng[3], Wan-Thai Hsu[3], and Sheng-Shian Li[1,4]

[1]Institute of NanoEngineering and MicroSystems, National Tsing Hua University, Hsinchu, Taiwan; [2]Industrial Technology Research Institute, Hsinchu, Taiwan; [3]TXC Corporation, Taoyuan, Taiwan; [4]Department of Power Mechanical Engineering, National Tsing Hua University, Hsinchu, Taiwan

ABSTRACT

A real-time aerosol sensor utilizing an SOI-MEMS thermal-piezoresistive oscillator (TPO) has been demonstrated in this work with sensor calibration using a commercial optical aerosol sensor (OAS). As compared to the self-sustained TPO [1], the DC power and operating temperature of the device can be significantly reduced by integrating the MEMS resonators and sustaining circuits, which leads to a longer lifetime and better reliability with lower power consumption and makes it a viable candidate for environmental sensing applications. The mass resolution of the proposed device is 3.34 fg extracted from a measured Allan deviation of 35 ppb, which is orders of magnitude higher than the commercially available quartz crystal microbalance (QCM). In addition, the proposed TPO technology also benefits cost reduction through the SOI-MEMS batch process as compared to its optical counterparts. Finally, the particulate matter (PM) sensing measurement under oxide (solid-phase PM_1, 1μm diameter) and smoke (liquid-phase PM_1, 1μm diameter) has shown a high correlation between the frequency slope of the TPO and the calibrated readings from the OAS.

INTRODUCTION

Exposure to outdoor air pollution has been confirmed to adversely affect human health because of the floating particulate matters (i.e., aerosols), which causes many diseases, such as cardiovascular disease and lung cancer [2][3]. One major harmful particulate matter group, named $PM_{2.5}$, is defined as particulates with diameter of 2.5μm or less, which can deeply damage the respiratory system [4] of the human beings. In order to measure the $PM_{2.5}$ concentrations in the environment for public health, optical aerosol sensors (OAS) are widely adopted with warranted accuracy. To further improve the sensing resolution with reduced system size and power consumption, new technologies are necessitated to target the portable personal healthcare systems.

In the current technology, the quartz crystal microbalance (QCM) is one of the candidates for such an aerosol sensing system. It provides low power operation feature and low cost, but suffers the low resolution characteristic for $PM_{2.5}$ and PM_1 particles. On the other hand, the micro-electro-mechanical systems (MEMS) based particle sensors are much more promising for the next-generation aerosol sensors because of their high sensitivity, low power consumption, excellent resolution, and small form factor. Many efforts have been devoted in the past 10 years for improving the performance of the MEMS-based aerosol sensors.

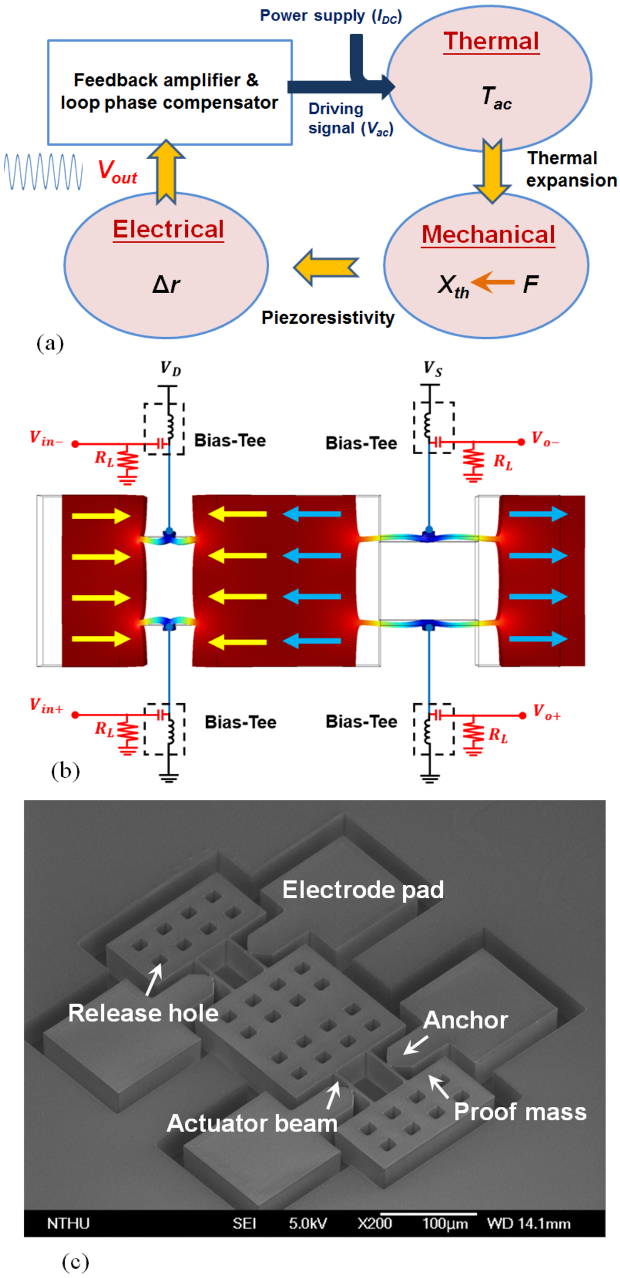

Figure 1: (a) Schematic of the feedback circuit-assisted thermo-electro-mechanical MEMS oscillator. (b) Operation of the proposed thermal-piezoresistive resonator array with its finite-element simulated mode shape. (c) SEM view of the thermal-piezoresistive resonator array fabricated in this work.

In this work, we developed a novel aerosol sensor based on a fully-differential thermal-piezoresistive resonator (TPR) oscillator. External phase locked loop

(PLL) based feedback amplifier is adopted for realizing the oscillation loop used in a real-time aerosol concentration tracking. The proposed aerosol sensor achieves a mass resolution of 3.34 fg, which is orders of magnitude better than the QCM sensors in the market.

WORKING PRINCIPLE

Amplifier-Assisted Thermal-Piezoresistive Oscillator

Unlike the self-sustained oscillation demonstrated in [1], external amplifier circuit is incorporated into the thermal-piezoresistive oscillator (TPO) loop in this work to reduce the biasing current, as shown in Fig. 1(a). The feedback amplifier provides additional gain and phase shift to fulfill the self-oscillation condition. Compared with [5][6], the dc biasing current (I_D) required for successful oscillation can be greatly reduced thanks to the help of external amplifier.

As shown in Fig. 1(b), the TPR used in this study is an II-shaped bulk acoustic resonator (II-BAR) array [7] which is fabricated using an SOI-MEMS process where its structural material is single crystal silicon (SCS) with negative piezoresistive coefficient (n-type doping). The array design is superior to the traditional II-BAR resonators [8][9] because of its fully differential actuation and sensing scheme for resistive feedthrough and common-mode noise rejection. This unique feature greatly improves the signal-to-background ratio (SBR) and produces doubled output signal power. The transconductance (g_m) of the II-BAR resonator array can be described as

$$g_m = 4\frac{E I_D I_S Q \alpha \pi_l}{C_{th}\omega_o} \tag{1}$$

where E is the elastic modulus of the silicon, Q is the quality factor, α is the thermal expansion coefficient, π_l is the longitudinal piezoresistive coefficient, C_{th} is the thermal capacitance of the actuator beam, ω_o is the resonance frequency, and I_D and I_S are the biasing currents for the actuation and sensing branches, respectively. Apparently, the transconductance of the array design is doubled as compared with single II-BAR. In addition, the array design also increases the proof-mass area for aerosal landing. The SEM picture of the fabricated resonator is shown in Fig. 1(c).

Mass Sensing Mechanisms

The oscillation frequency of the TPO can be described by the lumped mass-spring-damper frequency equation as

$$f_o = \frac{1}{2\pi}\sqrt{\frac{k}{m}} \tag{2}$$

where k and m are the effective stiffness and effective mass of the resonator, respectively. As the aerosols land on the resonator structure, it would not only increase the mass (Δm) but also influence the equivalent stiffness (Δk). Therefore, the shifts in the oscillation frequency can be described in a general form as

$$\Delta f = \frac{f_o}{2}\left(\frac{\Delta k}{k} - \frac{\Delta m}{m}\right) \tag{3}$$

For the aerosols attached to the proof-masses of the resonator, the change in stiffness would be minimized, and thus the mass sensitivity could be further simplified as

$$\frac{\Delta f}{f_o} \approx -\frac{\Delta m}{2m} \tag{4}$$

Eq. (4) is used to extract the added mass from the shifted oscillation frequency in this work.

EXPERIMENTAL SETUP

Fig. 2 illustrates the oscillator schematic of the II-BAR array connected with its sustaining circuits. To characterize the TPO performance, a table-top instrumentation setup is adopted for flexibility. The feedback sustaining circuit is implemented using a commercial lock-in amplifier (HF2LI-PLL, Zurich Instruments). In this setup, four bias tees are used to separate the ac and dc signals, and two power splitters are adopted to differentially actuate/sense the MEMS resonator array. The driving ac signal from the PLL is set below the bifurcation limit of the MEMS resonator array to prevent nonlinear operation. A frequency counter (Keysight 53230A) is utilized to record the oscillator frequency drift.

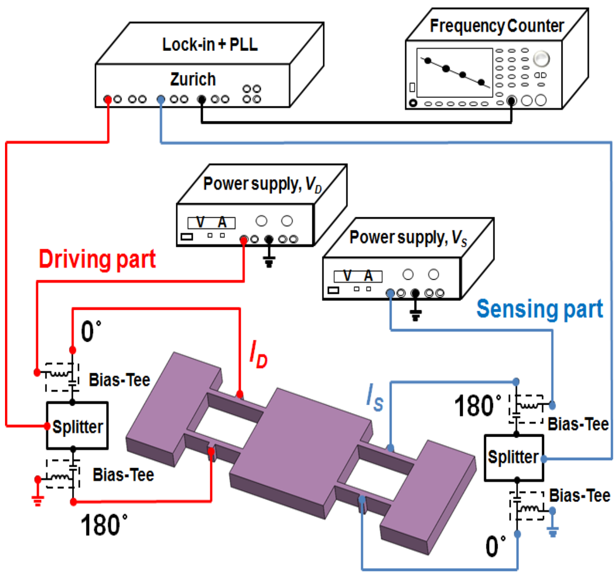

Figure 2: Schematic of an II-BAR array interfaced with its sustaining circuitry (Lock-in + PLL).

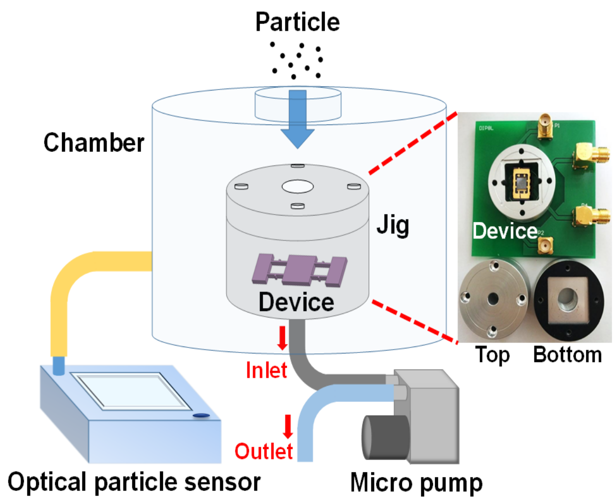

Figure 3: Measurement setup of the proposed aerosol sensor utilizing an SOI-MEMS TPO.

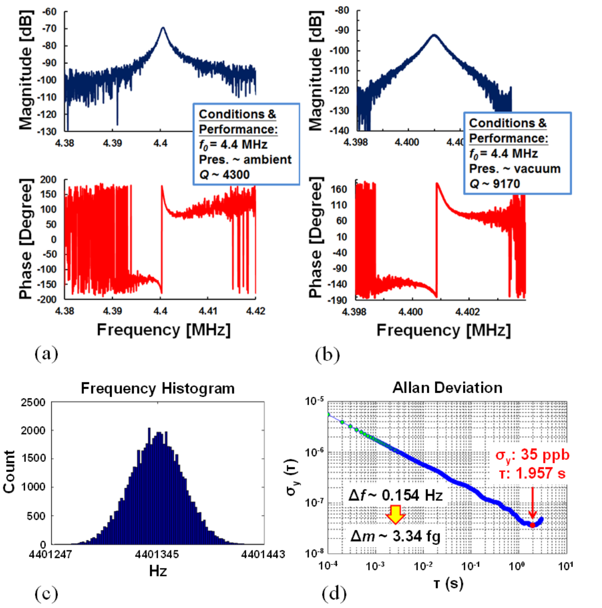

Figure 4: Frequency characteristics of a fully-differential TPR measured by a network analyzer, showing (a) Q of 4,300 in ambient pressure ($I_D + I_S$ = 70 mA) and (b) Q of 9,170 in vacuum chamber ($I_D + I_S$ = 40 mA). (c) Frequency counter measurement of the TPO in ambient pressure exhibits frequency fluctuation less than 200 Hz (3σ) and (d) Allan deviation of 35 ppb, which corresponds to a minimum detectable frequency variation of 0.154 Hz and mass resolution of 3.34 fg.

Fig. 3 presents the measurement setup of a silicon-based MEMS TPO aerosol sensor with real-time particle concentration monitoring using the OAS (Model: TSI 8533) as a standard calibrator. To perform the measurement, a micro-pump is utilized to drag chamber air consisting of the particles into the cylindrical jig to allow particles to impact and land onto the TPO through the flow momentum. Furthermore, the micro pump flow velocity calibration is carried out before the aerosol measurement.

There are mainly two categories of the ambient aerosol based on its physical properties, including solid particles (e.g., oxide) and liquid droplets (e.g., smoke). Therefore, our measurement setup depicted in Fig. 3 also focuses on these two types at PM_1 level (particle diameter equal or less than 1μm).

RESULTS AND DISCUSSION

Resonator and Oscillator Characterizations

Fig. 4(a) and (b) show the measured frequency characteristics of the fully-differential TPR array using a network analyzer (NA) under ambient pressure (P = 760 Torr) and high vacuum (P < 1 mTorr), respectively. Quality factor (Q) of 4,300 is recorded in ambient pressure while Q of 9,170 in vacuum. Apparently, compared with traditional single II-BAR resonators [8][9], the resistive feedthrough signal are completely cancelled in real time owing to the differential operation [7].

Prior to the particle sensing experiment, the frequency stability of the oscillator and the minimum measurable frequency variation are characterized using a frequency

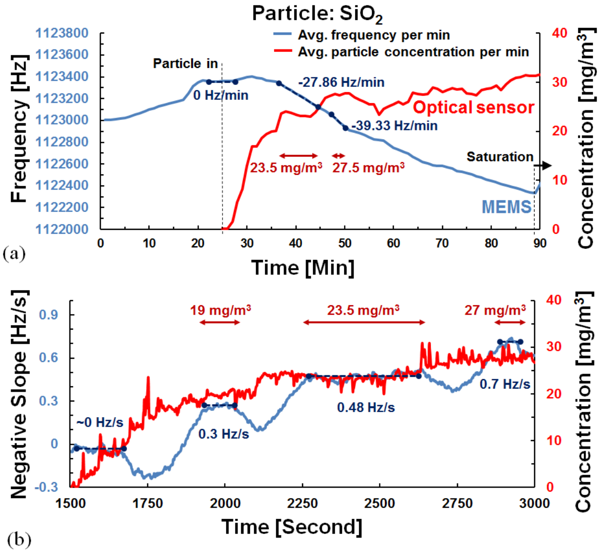

Figure 5: (a) PM_1 aerosol measurement result using solid particle (oxide), illustrating the relationship between the resonance frequency of the MEMS TPO and the particle concentration measured by the OAS. (b) Negative slope of the TPO resonance frequency is correlated to the OAS measurement result.

counter in the ambient pressure, as shown in Fig. 4(c) and (d), respectively. The gate time of 100 μs is selected to determine the short-term stability of the device. Measured frequency fluctuation (3σ confidence level) is within 200 Hz and the Allan deviation is less than 35 ppb with integration time of 1.95s. Based on the designed parameters, such a frequency inaccuracy is equivalent to a minimum detectable mass resolution of 3.34 fg.

Mass Sensor Characterizations

PM_1 silicon dioxide was selected as the first testing subject to represent the solid aerosol particles in the atmospheric environment. The measured TPO frequency affected by the oxide particles is presented in Fig. 5(a) while Fig. 5(b) shows the comparison of the TPO frequency slope versus the OAS calibration readings. After turning on the micro-pump to introduce particles onto the TPO sensor, its resonance frequency decreases steadily (cf. Fig. 5(a)) in correspondence with the oxide concentration in the chamber, until device saturation is reached. It can be observed that the resonance frequency of the element has a fairly consistent trend with the particle concentration. From the beginning, the drift of 0 Hz/min indicates that no particles are deposited on the surface of the MEMS until the frequency decreases by a rate of 27.86 Hz/min and 39.33 Hz/min, respectively, which correspond to the concentrations of 23.5 mg/m³ and 27.5 mg/m³ of the OAS readings, respectively.

In order to directly compare the MEMS readouts and the OAS calibration results, we convert the measurement results of the MEMS devices into the slopes (in Hz/s). The four different frequency slopes of the TPO labeled in Fig. 5(b) agree well with the OAS readings. It is shown that the change of the particle concentration is reflected in the oscillation frequency. As the oxide concentration of the test chamber gradually rises according to the OAS readings, the frequency slope (absolute value) extracted from the

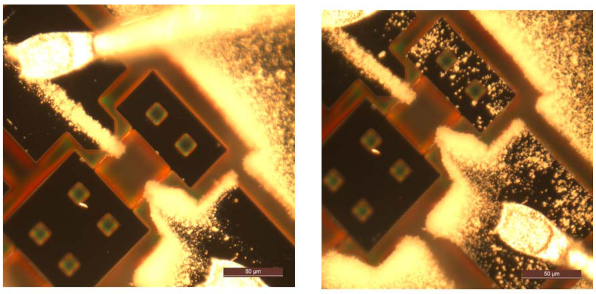

(a) (b)

Figure 6: Resonator OM views after (a) oxide particle and (b) smoke particle sensing.

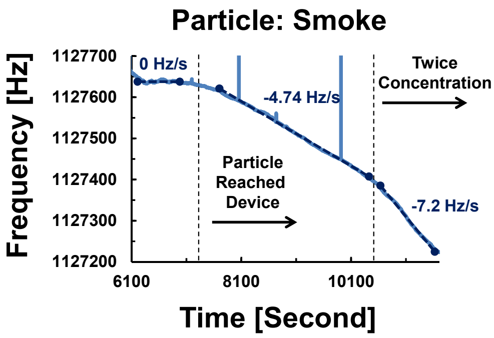

Figure 7: Resonance frequency drift of the proposed TPO under different smoke concentrations.

TPO becomes higher, thus verifying the efficacy of the proposed TPO particle sensor. Note that the discontinuous slope existed in Fig. 5(b) (i.e., the depression of the blue line) corresponds to the concentration change of the oxide particles. It is presumed that the oxide particles fall off the MEMS structure, but return to the corresponding slope with the stabilization of the environmental concentration.

In fact, the PM_1 oxide deposition mainly accumulated on the actuator beam and the anchor tip of the TPO limits the sensitivity and resolution of the proposed particle sensor, as shown in Fig. 6(a). The oxide particles cannot successfully land on the resonator proof mass due to the thermophoresis phenomenon. The region near the anchor part is the cold zone compared to the proof-masses, thus making the aerosol particles easier to sit at the actuator beam near the anchor tip. For this reason, the liquid phase aerosol (i.e., smoke) is used as the second testing subject since it is easier to overcome the thermophoresis phenomenon. The OM view presented in Fig. 6(b) right after the smoke deposition shows uniform distribution of particles on the top surface of the TPO proof-mass.

The smoke measurement in Fig. 7 shows two frequency slopes that correspond to different particle concentrations. As the particles land on the device, the frequency slope (absolute value) first remains constant at a rate of 4.74 Hz/s and then increases to 7.2 Hz/s under ~2X higher smoke concentration. It was postulated that a portion of the smoke particles were attached to the inner sidewall of the vacuum jig, so the frequency reduction rate is not doubled with the expectation.

CONCLUSION

An aerosol particle sensor utilizing the PLL-assisted TPO fabricated by a standard SOI-MEMS process was successfully demonstrated. For the open loop response, the quality factor of 4,300 in ambient pressure and 9,170 in vacuum was achieved. The Allan deviation of 35 ppb for the proposed aerosol sensor was measured in ambient pressure, which is equivalent to a minimum mass resolution of 3.34 fg. The SiO_2 and smoke particles can be successfully detected by the proposed TPO aerosol sensor. In the future, lower aerosol concentration measurement will be conducted to investigate the sensing limit of the proposed TPO.

ACKNOWLEDGEMENTS

This research was sponsored by the Ministry of Science and Technology (MOST-104-2622-E-007-009-CC2). The authors would like to thank ITRI for support of the measurement environment, and we also appreciate TXC Corporation for the technology advisory.

REFERENCES

[1] E.-C. Chang *et al.*, "Real-time mass sensing and dynamic impact monitoring …," *Proc., 29th Int. Conf. IEEE Micro Electro Mechanical Systems (MEMS'16)*, Jan. 24-28, 2016, pp. 1078-1081.

[2] P. Sallis *et al.*, "Air pollution and fog detection through vehicular sensors," *Proc., 8th Asia Modelling Symp. (AMS'14)*, Sep. 2014, pp. 181-186.

[3] C. A. Pope and D. W. Dockery, "Health effects of fine particulate air pollution: linesthat connect," *J. Air Waste Management Association*, vol. 56, no. 6, pp. 709-742, 2006.

[4] P. A. Solomon *et al.*, "Macroscopic to microscopic scales of particle dosimetry: from source to fate in the body," *Air Quality Atmosphere Health*, vol. 5, pp. 169-187, 2012.

[5] H. J. Hall *et al.*, "Mode selection behavior of VHF thermal-piezoresistive self-sustained oscillators," *17th Int. Conf. IEEE Solid-State Sensors, Actuators Microsystem (Transducers'13)*, June 16-20, 2013, pp. 1392-1395.

[6] A. Rahafrooz and S. Pourkamali, "Fully micromechanical piezo-thermal oscillators," *Proc., IEEE Int. Electron Device Meeting (IEDM'10)*, Dec. 2010, pp. 1-4.

[7] C.-C. Chen *et al.*, "Thermally-actuated and piezoresistively-sensed CMOS-MEMS …," *Proc., IEEE Int. Freq. Contr. Symp. (IFCS'10)*, May 21-24, 2012, pp. 443-446.

[8] A. Rahafrooz and S. Pourkamali, "High-frequency thermally actuated electromechanical resonators with piezoresistive readout," *IEEE Trans. Electron Devices*, vol. 58, no. 4, pp. 1205-1214, April 2011.

[9] A. Rasouli *et al.*, "Employing piezojunction effect for ultra-low power resonant microdevice applications," *Proc., 18th Int. Conf. IEEE Solid-State Sensors, Actuators Microsystem (Transducers'15)*, Aug. 2015, pp. 2021-2024.

CONTACT

*T.-Y. Liu, tel: +886-3-571-5131#80629;
emily5502907@gmail.com